Perturbational formulation of principal component analysis in molecular dynamics simulation

Yohei M. Koyama,[1,2,*] Tetsuya J. Kobayashi,[3,1] Shuji Tomoda,[2] and Hiroki R. Ueda[1,4,5,†]
[1]*Laboratory for Systems Biology, Center for Developmental Biology, RIKEN, 2-2-3 Minatojima-minamimachi, Chuo-ku, Kobe, Hyogo 650-0047, Japan*
[2]*Department of Life Sciences, Graduate School of Arts and Sciences, University of Tokyo, Komaba, Meguro-ku, Tokyo 153-8902, Japan*
[3]*Institute of Industrial Science, The University of Tokyo, 4-6-1 Komaba, Meguro-ku, Tokyo 153-8505, Japan*
[4]*Functional Genomics Unit, Center for Developmental Biology, RIKEN, 2-2-3 Minatojima-minamimachi, Chuo-ku, Kobe, Hyogo 650-0047, Japan*
[5]*Department of Bioscience, Graduate School of Science, Osaka University, Toyonaka, Osaka 560-0043, Japan*
(Received 31 May 2008; revised manuscript received 18 August 2008; published 7 October 2008)

Conformational fluctuations of a molecule are important to its function since such intrinsic fluctuations enable the molecule to respond to the external environmental perturbations. For extracting large conformational fluctuations, which predict the primary conformational change by the perturbation, principal component analysis (PCA) has been used in molecular dynamics simulations. However, several versions of PCA, such as Cartesian coordinate PCA and dihedral angle PCA (dPCA), are limited to use with molecules with a single dominant state or proteins where the dihedral angle represents an important internal coordinate. Other PCAs with general applicability, such as the PCA using pairwise atomic distances, do not represent the physical meaning clearly. Therefore, a formulation that provides general applicability and clearly represents the physical meaning is yet to be developed. For developing such a formulation, we consider the conformational distribution change by the perturbation with arbitrary linearly independent perturbation functions. Within the second order approximation of the Kullback-Leibler divergence by the perturbation, the PCA can be naturally interpreted as a method for (1) decomposing a given perturbation into perturbations that independently contribute to the conformational distribution change or (2) successively finding the perturbation that induces the largest conformational distribution change. In this perturbational formulation of PCA, (i) the eigenvalue measures the Kullback-Leibler divergence from the unperturbed to perturbed distributions, (ii) the eigenvector identifies the combination of the perturbation functions, and (iii) the principal component determines the probability change induced by the perturbation. Based on this formulation, we propose a PCA using potential energy terms, and we designate it as potential energy PCA (PEPCA). The PEPCA provides both general applicability and clear physical meaning. For demonstrating its power, we apply the PEPCA to an alanine dipeptide molecule in vacuum as a minimal model of a nonsingle dominant conformational biomolecule. The first and second principal components clearly characterize two stable states and the transition state between them. Positive and negative components with larger absolute values of the first and second eigenvectors identify the electrostatic interactions, which stabilize or destabilize each stable state and the transition state. Our result therefore indicates that PCA can be applied, by carefully selecting the perturbation functions, not only to identify the molecular conformational fluctuation but also to predict the conformational distribution change by the perturbation beyond the limitation of the previous methods.

DOI: 10.1103/PhysRevE.78.046702 PACS number(s): 02.70.Rr, 36.20.Ey, 87.15.ap, 89.70.Cf

I. INTRODUCTION

Conformational fluctuations of a molecule are important to its function, since such intrinsic fluctuations enable the molecule to respond to perturbations in the external environment [1,2]. For extracting a large conformational fluctuation, which is believed to relate to the primary conformational change by the perturbation, principal component analysis (PCA) [3], also called essential dynamics, has been generally used in molecular dynamics (MD) simulations [4–8]. In general, PCA is performed using Cartesian coordinates. Since Cartesian coordinates depend on the overall molecular motion, translational and rotational motion have to be eliminated before the calculation of the covariance matrix. Molecular translation can be eliminated uniquely by translating the molecular center of mass to the origin. However, molecular rotation cannot be removed uniquely by least square fitting to a certain reference structure, except the molecule fluctuating around the single dominant state. This is because the fitting result generally depends on the selected reference structure [9–11]. We refer to this problem as "frame fitting problem" in this study. To avoid the frame fitting problem, several PCAs using internal coordinates, which is independent of the overall molecular motion, have been proposed such as the dihedral angle PCA (dPCA) [12,13] and a PCA using pairwise atomic distances [11]. The dihedral angle represents an important internal coordinate for proteins. However, it is difficult to apply the dPCA to other molecules such as nucleic acids. PCA using pairwise atomic distances have general applicability, but their physical meaning is unclear. Furthermore, these methods do not directly relate the identified large conformational fluctuations with the conformational change induced by the environmental perturbation such as ligand binding. Therefore, a formulation for charac-

*ym.koyama@gmail.com
†uedah-tky@umin.ac.jp

terizing conformational fluctuations, which (a) achieves general applicability, (b) describes its physical meaning, and (c) predicts the conformational change by the perturbation is unavailable.

Some previous studies more directly tried to relate conformational fluctuations with the conformational change induced by the environmental perturbation. Ikeguchi *et al.* [14] applied linear response theory for predicting the average conformational change induced by constant force perturbations from the covariance matrix of atomic coordinates in an unperturbed equilibrium state. Because they used Cartesian atomic coordinates, their method also inherits the frame fitting problem as in the case of Cartesian PCA, which limits its applicability to molecules with a single dominant state. Ming *et al.* [15,16] proposed quantifying the conformational distribution change by the perturbation with the Kullback-Leibler divergence. They used the harmonic approximation of the unperturbed and the perturbed energy function, i.e., normal mode approximation, in which each equilibrium distribution becomes a multivariate normal distribution. By this approximation, they estimate the Kullback-Leibler divergence by deriving its analytical expression. Although applications of the Kullback-Leibler divergence are not limited to the multivariate normal distributions, the normal mode approximation limits their method to conformational change from a single-dominant state to another single-dominant state by the perturbation. Therefore, a formulation that satisfies the above mentioned three requirements (a)–(c) is still not available.

For developing such a formulation, we first introduce a perturbation with arbitrary linearly independent perturbation functions (Sec. II A). We then quantify the conformational distribution change by the Kullback-Leibler divergence, which is naturally derived from large deviation theory (Sec. II B). Within the second order approximation of the Kullback-Leibler divergence, the PCA can be naturally interpreted as a method for (1) decomposing a given perturbation into perturbations that independently contribute to the conformational distribution change or (2) successively finding the perturbation that induces the largest conformational distribution change (Sec. II C). We then propose a PCA using potential energy terms, which is designated as potential energy PCA (PEPCA). The PEPCA gives general applicability and clear physical meaning (Sec. II D). For demonstrating its power, we apply the PEPCA to an alanine dipeptide molecule in vacuum as a minimal model of a nonsingle dominant conformational biomolecule (Sec. III). Finally, we discuss the theoretical implications of our perturbational formulation of PCA, and the applicability of the PEPCA to larger molecules (Sec. IV).

II. THEORY

A. Perturbation of a molecular system

We consider a molecular system that is described by the potential energy $V(\mathbf{q})$, where $\mathbf{q}=(q_1,\ldots,q_{3N})^T$ are the atomic Cartesian coordinates and N is the number of atoms. Then, the canonical distribution $\rho(\mathbf{q})$ at temperature T is

$$\rho(\mathbf{q}) = \frac{1}{Z} e^{-V(\mathbf{q})/k_B T}, \tag{1}$$

where k_B and Z are the Boltzmann constant and the partition function (normalizing constant), respectively. We perturb the molecular system using perturbation parameters $\boldsymbol{\lambda}=(\lambda_1,\ldots,\lambda_M)^T$ and linearly independent perturbation functions $\mathbf{f}(\mathbf{q})=[f_1(\mathbf{q}),\ldots,f_M(\mathbf{q})]^T$ as

$$V_{\boldsymbol{\lambda}}(\mathbf{q}) = V(\mathbf{q}) - k_B T \sum_{i=1}^{M} \lambda_i f_i(\mathbf{q}). \tag{2}$$

Then, the perturbed canonical distribution $\rho_{\boldsymbol{\lambda}}(\mathbf{q})$ is

$$\rho_{\boldsymbol{\lambda}}(\mathbf{q}) = \frac{1}{Z_{\boldsymbol{\lambda}}} e^{-V_{\boldsymbol{\lambda}}(\mathbf{q})/k_B T} = e^{\boldsymbol{\lambda}\cdot\mathbf{f}(\mathbf{q}) - \psi(\boldsymbol{\lambda})} \rho(\mathbf{q}), \tag{3}$$

where we define

$$\psi(\boldsymbol{\lambda}) \equiv \ln \frac{Z_{\boldsymbol{\lambda}}}{Z} = \ln \langle e^{\boldsymbol{\lambda}\cdot\mathbf{f}} \rangle, \tag{4}$$

and $\langle\cdots\rangle$ indicates the average under $\rho(\mathbf{q})$. We consider the $\boldsymbol{\lambda}$ region where $\psi(\boldsymbol{\lambda})$ exists. This representation enables us to consider the perturbed distribution [Eq. (3)] as an exponential family, which is broadly studied in statistics [17–21]. In the theory of the exponential family, $\boldsymbol{\lambda}$, $\mathbf{f}(\mathbf{q})$, and $\psi(\boldsymbol{\lambda})$ are called natural parameters, sufficient statistics, and cumulant generating function, respectively. The nth derivative of the cumulant generating function $\psi_{i_1\cdots i_n}(\boldsymbol{\lambda}_0) \equiv \frac{\partial^n \psi(\boldsymbol{\lambda})}{\partial\lambda_{i_n}\cdots\partial\lambda_{i_1}}\big|_{\boldsymbol{\lambda}=\boldsymbol{\lambda}_0}$ is known as the nth cumulant. In particular, the first cumulant is the average $\psi_i(\boldsymbol{\lambda})=\langle f_i\rangle_{\boldsymbol{\lambda}}$, and the second cumulant is the covariance $\psi_{ij}(\boldsymbol{\lambda})=\langle (f_i-\langle f_i\rangle_{\boldsymbol{\lambda}})(f_j-\langle f_j\rangle_{\boldsymbol{\lambda}})\rangle_{\boldsymbol{\lambda}}$, where $\langle\cdots\rangle_{\boldsymbol{\lambda}}$ indicates the average under $\rho_{\boldsymbol{\lambda}}(\mathbf{q})$. $\langle\cdots\rangle_0$ is equivalent to $\langle\cdots\rangle$.

B. Quantification of the conformational distribution change by the perturbation

For quantifying the conformational distribution change induced by the perturbation, we use the Kullback-Leibler divergence [15–17,21–24], which naturally appears in Sanov's theorem in large deviation theory [21,23,25,26], and is defined as

$$D(\rho_{\boldsymbol{\lambda}} \| \rho) \equiv \int \rho_{\boldsymbol{\lambda}}(\mathbf{q}) \ln \frac{\rho_{\boldsymbol{\lambda}}(\mathbf{q})}{\rho(\mathbf{q})} d\mathbf{q} \geqslant 0. \tag{5}$$

The Kullback-Leibler divergence is non-negative, equals zero if and only if two distributions are identical, and is generally asymmetric with respect to the exchange of the two distributions. Using Eq. (3), Eq. (5) is represented as

$$D(\rho_{\boldsymbol{\lambda}} \| \rho) = \boldsymbol{\lambda}\cdot\langle\mathbf{f}\rangle_{\boldsymbol{\lambda}} - \psi(\boldsymbol{\lambda}) = \sum_{i=1}^{M} \lambda_i \psi_i(\boldsymbol{\lambda}) - \psi(\boldsymbol{\lambda}). \tag{6}$$

By using the Taylor expansions of $\psi_i(\boldsymbol{\lambda})$ and $\psi(\boldsymbol{\lambda})$ around the origin, Eq. (6) is expanded as

$$D(\rho_{\boldsymbol{\lambda}}\|\rho) = \frac{1}{2}\sum_{i,j=1}^{M} \psi_{ij}(0)\lambda_i\lambda_j + \frac{1}{3}\sum_{i,j,k=1}^{M} \psi_{ijk}(0)\lambda_i\lambda_j\lambda_k + \cdots, \tag{7}$$

the nth order coefficient is $\frac{1}{(n-2)!n}$. The Kullback-Leibler divergence can also be represented by $\langle \mathbf{f} \rangle_{\boldsymbol{\lambda}}$ instead of $\boldsymbol{\lambda}$ as shown in Appendix A.

C. Perturbational formulation of principal component analysis

Here, we consider a PCA with respect to the conformational distribution change induced by the perturbations formulated in the preceding sections. We denote the covariance matrix of $\mathbf{f}(\mathbf{q})$ in an unperturbed distribution $\rho(\mathbf{q})$ as $\mathbf{C}$, where $C_{ij}=\psi_{ij}(0)=\langle (f_i-\langle f_i\rangle)(f_j-\langle f_j\rangle)\rangle$. Since the covariance matrix is a positive definite matrix [we assume each variance of $f_i(\mathbf{q})$ is nonzero, i.e., not constant], we can diagonalize the matrix using the orthogonal matrix $\mathbf{U}=(\mathbf{u}_1,\ldots,\mathbf{u}_M)$ and positive eigenvalues σ_i^2. We assume the eigenvalues are sorted in descending order. On the basis of the eigenvectors, the Kullback-Leibler divergence in the second order approximation [Eq. (7)] is represented as

$$D(\rho_{\boldsymbol{\lambda}}\|\rho) \approx \frac{1}{2}\boldsymbol{\lambda}^T\mathbf{C}\boldsymbol{\lambda} = \frac{1}{2}(\mathbf{U}^T\boldsymbol{\lambda})^T(\mathbf{U}^T\mathbf{C}\mathbf{U})(\mathbf{U}^T\boldsymbol{\lambda}) = \frac{1}{2}\sum_{i=1}^{M}\sigma_i^2\xi_i^2, \tag{8}$$

where we define

$$\boldsymbol{\xi} \equiv \mathbf{U}^T\boldsymbol{\lambda}, \tag{9}$$

which are the perturbation parameters corresponding to the eigenvectors. Thus, within the second order approximation of the Kullback-Leibler divergence, the given perturbation $\boldsymbol{\lambda}$ is decomposed into the perturbations ξ_i, which independently contribute to the Kullback-Leibler divergence by $\frac{1}{2}\sigma_i^2\xi_i^2$. Therefore, the eigenvalue σ_i^2 measures the conformational distribution change induced by the decomposed perturbation ξ_i. Components of the eigenvector $\mathbf{u}_i$ identifies the combinations of the perturbation functions that induces the decomposed perturbation ξ_i.

Since the covariance matrix is symmetric, the ith eigenvector $\mathbf{u}_i$ can be also characterized variationally as $\boldsymbol{\lambda}$, which maximizes $\boldsymbol{\lambda}^T\mathbf{C}\boldsymbol{\lambda}$ with constraints $|\boldsymbol{\lambda}|=\text{const}$ and $\mathbf{u}_j\cdot\boldsymbol{\lambda}=0$, $j=1,\ldots,i-1$ [3,27]. The second order approximation of the Kullback-Leibler divergence is in the quadratic form $\frac{1}{2}\boldsymbol{\lambda}^T\mathbf{C}\boldsymbol{\lambda}$. Therefore, we can interpret the diagonalization of the covariance matrix by successively finding the perturbation $\boldsymbol{\lambda}$ which maximizes the Kullback-Leibler divergence $D(\rho_{\boldsymbol{\lambda}}\|\rho)$ under the constraints

$$|\boldsymbol{\lambda}| = \delta, \quad \delta \text{ such that the second order, approximation of } D(\rho_{\boldsymbol{\lambda}}\|\rho) \text{ is valid,} \tag{10a}$$

$$\mathbf{u}_j\cdot\boldsymbol{\lambda} = 0, \quad j = 1,\ldots,i-1. \tag{10b}$$

Equivalently, it can be expressed as

$$\max_{\substack{|\boldsymbol{\lambda}|=\delta \\ \mathbf{u}_j\cdot\boldsymbol{\lambda}=0, j=1,\ldots,i-1}} D(\rho_{\boldsymbol{\lambda}}\|\rho) \approx \max_{\substack{|\boldsymbol{\lambda}|=\delta \\ \mathbf{u}_j\cdot\boldsymbol{\lambda}=0, j=1,\ldots,i-1}} \frac{1}{2}\boldsymbol{\lambda}^T\mathbf{C}\boldsymbol{\lambda} = \frac{1}{2}(\delta\mathbf{u}_i)^T\mathbf{C}(\delta\mathbf{u}_i) = \frac{1}{2}\delta^2\sigma_i^2. \tag{11}$$

From Eq. (3), the probability change of $\mathbf{q}$ induced by the perturbation $\boldsymbol{\lambda}$ can be represented as

$$\ln\frac{\rho_{\boldsymbol{\lambda}}(\mathbf{q})}{\rho(\mathbf{q})} = \boldsymbol{\lambda}\cdot\mathbf{f}(\mathbf{q}) - \psi(\boldsymbol{\lambda}) = \boldsymbol{\lambda}\cdot\mathbf{f}(\mathbf{q}) - \left(\langle\mathbf{f}\rangle\cdot\boldsymbol{\lambda} + \frac{1}{2}\boldsymbol{\lambda}^T\mathbf{C}\boldsymbol{\lambda} + \cdots\right) = \mathbf{g}(\mathbf{q})\cdot\boldsymbol{\xi} - \frac{1}{2}\sum_{i=1}^{M}\sigma_i^2\xi_i^2 - \cdots \tag{12}$$

$$= \sum_{i=1}^{M}\left(g_i(\mathbf{q})\xi_i - \frac{1}{2}\sigma_i^2\xi_i^2\right) - \cdots, \tag{13}$$

where we define $\mathbf{g}(\mathbf{q})=[g_1(\mathbf{q}),\ldots,g_M(\mathbf{q})]^T$ as

$$\mathbf{g}(\mathbf{q}) \equiv \mathbf{U}^T[\mathbf{f}(\mathbf{q}) - \langle\mathbf{f}\rangle]. \tag{14}$$

These functions $\mathbf{g}(\mathbf{q})$ can be considered as the principal components of $\mathbf{f}(\mathbf{q})$ under $\rho(\mathbf{q})$. Thus, in the second order approximation of the Kullback-Leibler divergence, the probability change induced by the perturbation ξ_i is determined only by the ith principal component $g_i(\mathbf{q})$ and the ith eigenvalue σ_i^2. Moreover, for the perturbation where the first order approximation of the cumulant generating function is valid, the probability change is determined only by the ith principal component. Perturbation $\xi_i>0$ increases the probability of $\mathbf{q}$ where $g_i(\mathbf{q})>0$, and decreases $\mathbf{q}$ where $g_i(\mathbf{q})<0$. Equation (14) indicates that these principal components $\mathbf{g}(\mathbf{q})$ are

$$\langle g_i\rangle = 0, \tag{15}$$

$$\langle g_i g_j\rangle = \sigma_i^2\delta_{i,j}. \tag{16}$$

Thus, the principal components make orthogonal functions with respect to the inner product

$$\langle g_i, g_j\rangle \equiv \int g_i(\mathbf{q})g_j(\mathbf{q})\rho(\mathbf{q})d\mathbf{q}. \tag{17}$$

In summary, in our perturbational formulation, within the second order approximation of the Kullback-Leibler divergence, the PCA can be interpreted as a method for (1) decomposing a given perturbation $\boldsymbol{\lambda}$ into perturbations that independently contribute to the conformational distribution change measured by the Kullback-Leibler divergence or (2) successively finding the perturbation that induces the largest conformational distribution change under the constraints [Eqs. (10)]. Then, (i) the eigenvalue σ_i^2 measures the Kullback-Leibler divergence by the perturbation ξ_i as $\frac{1}{2}\sigma_i^2\xi_i^2$ [Eq. (8)]. (ii) Eigenvector $\mathbf{u}_i$ identifies the combination of perturbation functions that induces the ith largest conformational distribution change. (iii) The principal component

$g_i(\mathbf{q})$ determines the probability change of $\mathbf{q}$ induced by the perturbation ξ_i [Eq. (13)]. In Appendix B, we give perturbational formulations of Cartesian PCA and dPCA.

D. Perturbation of potential energy terms

To develop a PCA that satisfies the three requirements (a)–(c) mentioned in the Introduction, we consider a perturbation of potential energy terms. We perturb some potential energy terms

$$\mathbf{V}(\mathbf{q}) = [V_1(\mathbf{q}), \ldots, V_M(\mathbf{q})]^T \tag{18}$$

in potential energy $V(\mathbf{q})$ with perturbation term in Eq. (2)

$$-k_B T \sum_{i=1}^{M} \lambda_i f_i(\mathbf{q}) = -\sum_{i=1}^{M} \lambda_i V_i(\mathbf{q}). \tag{19}$$

This perturbation changes the weight of the potential energy term V_i by $(1-\lambda_i)$. This gives perturbation functions

$$\mathbf{f}(\mathbf{q}) = \left(\frac{V_1(\mathbf{q})}{k_B T}, \ldots, \frac{V_M(\mathbf{q})}{k_B T} \right)^T. \tag{20}$$

Thus, a PCA using these perturbation functions (PEPCA) can be interpreted as a method for (1) decomposing a given potential energy terms perturbation [Eq. (19)] into perturbations that independently contribute to the conformational distribution change or (2) successively finding the potential energy terms perturbation [Eq. (19)] that induces the largest conformational distribution change under the constraints Eqs. (10). Since the potential energy terms are always defined in MD simulations, and they are invariant with respect to the overall molecular motion, the requirement (a) in the Introduction is satisfied. A potential energy term represents the molecular interaction, therefore, the requirement (b) is satisfied. The requirement (c) is automatically satisfied in our perturbational formulation.

Perturbation $\lambda_i = 1$ eliminates the potential energy term V_i. $\boldsymbol{\xi}$ corresponding to $\boldsymbol{\lambda} = (1, \ldots, 1)^T$ is

$$\boldsymbol{\xi} = \mathbf{U}^T \boldsymbol{\lambda} = \mathbf{U}^T (1, \ldots, 1)^T = \left(\sum_{i=1}^{M} U_{i1}, \ldots, \sum_{i=1}^{M} U_{iM} \right)^T. \tag{21}$$

We standardize the direction of the jth eigenvector $\mathbf{u}_j$ as $\Sigma_{i=1}^{M} U_{ij} \geqslant 0$ for convenience, because the direction of the eigenvector does not change the result. If we perturb ξ_j direction, i.e., $\boldsymbol{\lambda} = \xi_j \mathbf{u}_j$, then the perturbation term Eq. (19) is represented as

$$-\sum_{i=1}^{M} \lambda_i V_i(\mathbf{q}) = -\sum_{i=1}^{M} \xi_j U_{ij} V_i(\mathbf{q}). \tag{22}$$

Therefore the perturbation $\xi_j > 0$ strengthens the ith potential energy term V_i if $U_{ij} < 0$, and it weakens the term if $U_{ij} > 0$. As discussed in Sec. II C, perturbation $\xi_j > 0$ increases the probability of $\mathbf{q}$ if $g_j(\mathbf{q}) > 0$, and decreases it if $g_j(\mathbf{q}) < 0$, in the first order approximation of $\psi(\boldsymbol{\lambda})$. These results are summarized in Table I. Thus, we can identify the combination of potential energy terms stabilizing $\mathbf{q}$, where $g_j(\mathbf{q}) < 0$ by $U_{ij} > 0$, and $g_j(\mathbf{q}) > 0$ by $U_{ij} < 0$. Therefore, the magnitude and the sign of the eigenvectors provide important information in the PEPCA. Moreover, we can investigate the detailed information of potential energy term, such as attractive or repulsive electrostatic interaction.

TABLE I. Effects of the perturbation ξ_j in the potential energy terms perturbation. Change in the weight of the potential energy term V_i by ξ_j is determined by Eq. (22). The probability change of $\mathbf{q}$ by ξ_j is determined by Eq. (13). The term "increase" or "decrease" indicates the probability change in the first order approximation of the cumulant generating function $\psi(\boldsymbol{\lambda})$.

	potential energy term V_i		Probability of $\mathbf{q}$	
	$U_{ij} > 0$	$U_{ij} < 0$	$g_j(\mathbf{q}) > 0$	$g_j(\mathbf{q}) < 0$
$\xi_j > 0$	weaken	strengthen	increase	decrease
$\xi_j < 0$	strengthen	weaken	decrease	increase

Next, we consider some concrete potential energy terms to perturb. Currently, the most commonly used biomolecular potential energy [28] has a functional form

$$\begin{aligned} V(\mathbf{q}) = & \sum_{b \in \text{bonds}} K_b (r_b - \bar{r}_b)^2 + \sum_{a \in \text{angles}} K_a (\theta_a - \bar{\theta}_a)^2 \\ & + \sum_{d \in \text{dihedrals}} K_d [\cos(n_d \varphi_d - \gamma_d) + 1] \\ & + \sum_{(i,j) \in \text{nonbonds}} \left(\frac{A_{ij}}{r_{ij}^{12}} - \frac{B_{ij}}{r_{ij}^{6}} \right) + \sum_{(i,j) \in \text{nonbonds}} \frac{Q_i Q_j}{\varepsilon r_{ij}}. \end{aligned} \tag{23}$$

Each term corresponds to the bond, angle, dihedral, van der Waals, and electrostatic potential energy terms, respectively. We can select all or some (e.g., nonbonded interactions only) of the potential energy terms to perturb as

$$\begin{aligned} \mathbf{V}(\mathbf{q}) = \Bigg(& \{K_b (r_b - \bar{r}_b)^2 | b \in \text{some bonds}\}, \\ & \{K_a (\theta_a - \bar{\theta}_a)^2 | a \in \text{some angles}\}, \\ & \{K_d (\cos(n_d \varphi_d - \gamma_d) + 1) | d \in \text{some dihedrals}\}, \\ & \left\{ \frac{A_{ij}}{r_{ij}^{12}} - \frac{B_{ij}}{r_{ij}^{6}} | (i,j) \in \text{some nonbonds} \right\}, \\ & \left\{ \frac{Q_i Q_j}{\varepsilon r_{ij}} | (i,j) \in \text{some nonbonds} \right\} \Bigg)^T. \end{aligned} \tag{24}$$

III. NUMERICAL RESULTS

For demonstrating the power of the theory, we apply the PEPCA to an alanine dipeptide molecule in vacuum. We performed 10 ns molecular dynamics simulation by integration with a 2 fs time step. For generating a canonical ensemble at 300 K, Langevin dynamics with the collision frequency $\gamma = 1.0\ \text{ps}^{-1}$ were used. We used molecular dynamics package AMBER8 [29] to perform molecular dynamics simulation and

TABLE II. Index of the potential energy terms of the alanine dipeptide. 89, 90, 101, and 102 are the improper torsion potential energy terms. 236–276 van der Waals and 410–450 electrostatic potential energy terms are 1–4 interactions, and they are divided by 2.0 and 1.2 (these are default values in AMBER8 [29]), respectively.

Bond	Angle	Dihedral	van der Waals	Electrostatic
1–21	22–57	58–102	103–276	277–450

the ff03 force field [30] which has the functional form given in Eq. (23). We saved the coordinates at every 1 ps, and used a total of 10,000 coordinates for the analysis. This molecule has two stable states in our 10 ns simulation. The transition between the two states occurred many times, and it equilibrated well within the two states. For performing the PEPCA, we developed a program that outputs the potential energy terms from the topology and coordinates files. We use all the potential energy terms for Eq. (18), and index each of them as in Table II. As indicated in Eq. (20), all potential energy terms are divided by k_BT for PCA. PCA was performed with the statistical computing environment R [31].

Figure 1 shows the eigenvalues of the covariance matrix of the potential energy terms divided by k_BT. The largest eigenvalue σ_1^2 is remarkably larger than the other eigenvalues. The second order approximation of the Kullback-Leibler divergence is represented as Eq. (8). Therefore, the perturbation corresponding to the largest eigenvalue changes the conformational distribution remarkably, and the other perturbations have less effect on the conformational distribution.

Therefore, we concentrate on analyzing the largest perturbation ξ_1. Figure 2(a) shows the sign of the first principal component $g_1(\mathbf{q})$ on a Ramachandran plot, which clearly characterizes the two stable states. As summarized in Table I, the perturbation $\xi_1>0$ increases the probability of $\mathbf{q}$ where

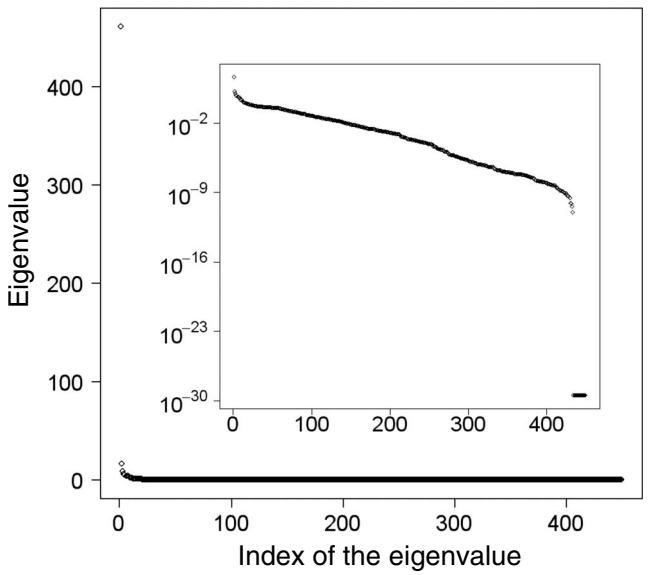

FIG. 1. Eigenvalues of the covariance matrix of the potential energy terms divided by k_BT. Eigenvalues are sorted in descending order. The inset figure shows the eigenvalues in log scale. First five eigenvalues are 461.5, 16.3, 9.3, 5.7, and 5.3.

$g_1(\mathbf{q})>0$ [red in Fig. 2(a)], and decreases the probability of $\mathbf{q}$, where $g_1(\mathbf{q})<0$ [blue in Fig. 2(a)], in the first order approximation. Therefore, the perturbation ξ_1 controls the ratio of the two stable states. As summarized in Table I, we can identify the combination of interactions stabilizing the conformation $\mathbf{q}$, where $g_1(\mathbf{q})>0$ [red in Fig. 2(a)] as the negative components of the first eigenvector ($U_{i1}<0$). In details, according to Table I, we first notify that the probability of the conformation $\mathbf{q}$, where $g_1(\mathbf{q})>0$ increases if $\xi_1>0$. We then notify that the potential energy term V_i is strengthened under $\xi_1>0$ if $U_{i1}<0$. We thus identify the interactions ($U_{i1}<0$) which stabilize the conformation $\mathbf{q}$ where $g_1(\mathbf{q})>0$. Figure 2(b) shows that smaller negative components of the first eigenvector are el-6-17, el-5-18, and el-8-16. According to Table III, el-8-16 is an attractive interaction while el-6-17 and el-5-18 are repulsive interactions. Conformation A [Figs. 2(a) and 2(b)] ascertains that the attractive interaction el-8-16 is an important stabilizing interaction. Interestingly, the conformation A also indicates that the extended β-like structure is enhanced by repulsive interactions el-6-17 and el-5-18. Similarly, the positive components of the first eigenvector ($U_{i1}>0$) stabilizes the conformation $\mathbf{q}$, where $g_1(\mathbf{q})<0$ [blue in Fig. 2(a)]. The larger positive component el-6-18 is an attractive interaction [Figure 2(b) and Table III]. Conformation B [Figs. 2(a) and 2(b)] ascertains that the attractive interaction el-6-18 is an important stabilizing interaction. Thus, the perturbation ξ_1 controls the ratio of the two stable states, i.e., the equilibrium constant of the two stable states. The negative and the positive components of the first eigenvector clearly identifies the stabilizing interactions of the two stable states.

Next, we analyze the second largest perturbation ξ_2, although its effect is smaller compared with that of the largest perturbation ξ_1. Figure 2(c) shows the sign of the second principal component $g_2(\mathbf{q})$. Interestingly, $g_2(\mathbf{q})$ clearly characterizes the transition state region of the two stable states. Therefore, the perturbation ξ_2 controls the ratio between the transition state and the two stable states. The smaller negative components of the second eigenvector ($U_{i2}<0$), which stabilize the conformation $\mathbf{q}$ where $g_2(\mathbf{q})>0$ [red in Fig. 2(c)], are attractive interactions el-5-16 and el-6-15 [Figure 2(d) and Table III]. Conformation TS [Figs. 2(c) and 2(d)] ascertains that attractive interactions el-5-16 and el-6-15 are important stabilizing interactions. On the other hand, the large positive component of the second eigenvector ($U_{i2}>0$), which stabilizes the conformation $\mathbf{q}$ where $g_2(\mathbf{q})<0$ [blue in Fig. 2(c)], is a repulsive interaction el-6-16 [Figure 2(d) and Table III]. The conformation TS indicates that the repulsive interaction el-6-16 destabilizes the transition state. Therefore, el-6-16 relatively stabilizes the two stable states [blue in Fig. 2(c)] by destabilizing the transition state [red in Fig. 2(c)]. Thus, the second largest perturbation ξ_2 controls the stability of the transition state of the two stable states, i.e., the rate constant of the transition between the two stable states. The negative and the positive components of the second eigenvector identify the stabilizing interactions of the transition state and the two stable states.

IV. DISCUSSION AND CONCLUSIONS

In this study, we clarified that within the second order approximation of the Kullback-Leibler divergence, a PCA

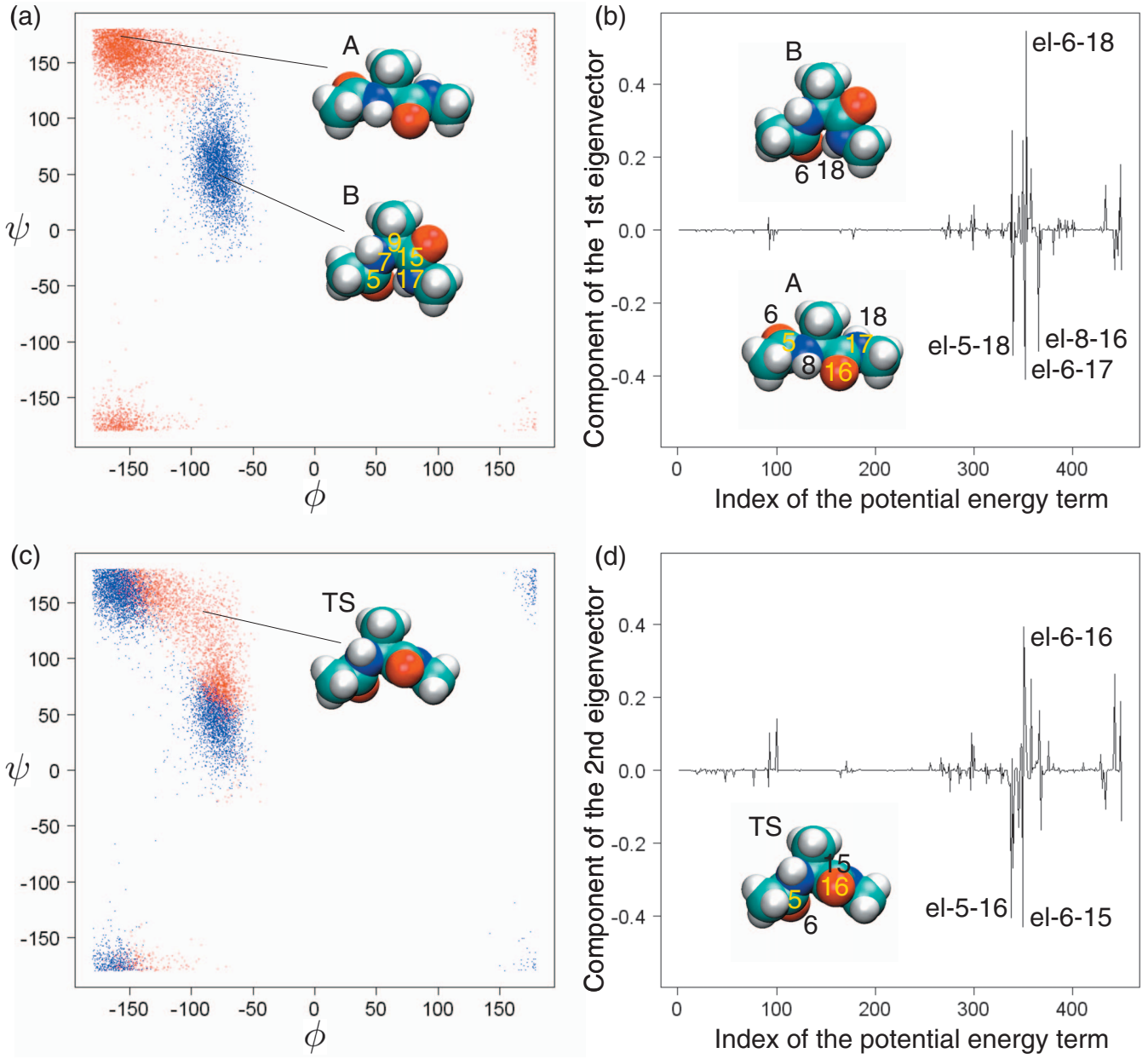

FIG. 2. (Color) The sign of (a) the first $[g_1(\mathbf{q})]$ and (c) the second $[g_2(\mathbf{q})]$ principal component on a Ramachandran plot. Red and blue points show $g_i(\mathbf{q}) \geq 0$ and $g_i(\mathbf{q}) < 0$, respectively. The dihedral angles ϕ and ψ are defined by atom indices 5-7-9-15 and 7-9-15-17, respectively. The 3D structures labeled A, B, and TS show snapshots of the MD simulation indicated by the black lines. The 3D structures were rendered by VMD [32]. Cyan, white, red, and blue spheres indicate the C, H, O, and N atoms, respectively. The components of (b) the first and (d) the second eigenvectors. Label el-6-18 indicates the component of the electrostatic potential energy term between atom 6 and atom 18. Such labels are captioned where the absolute value of the component is larger than 0.3.

can be interpreted as a method for (1) decomposing a given perturbation into perturbations that independently contribute to the conformational distribution change or (2) successively finding the perturbation that induces the largest conformational distribution change. To achieve general applicability and provide clear physical meaning of the perturbation, we introduced a perturbation of potential energy terms, which leads to the PEPCA. The effectiveness of the PEPCA was demonstrated using alanine dipeptide as a minimal model of a nonsingle dominant state behavior biomolecule.

TABLE III. Charge (electron charge units) of the numbered atoms in Figs. 2(b) and 2(d).

5(C)	6(O)	8(H)	15(C)	16(O)	17(N)	18(H)
0.512	−0.550	0.294	0.570	−0.555	−0.424	0.290

To apply the PEPCA to larger molecules, we must investigate some practical aspects that were not addressed in this paper. First, water molecules are not incorporated in our MD simulation. For more practical simulation, it is important to explicitly incorporate water molecules in MD simulation.

Here we represent the biomolecular coordinates $\mathbf{q}$ and the water coordinates $\mathbf{q}'$. If we only perturb the biomolecules, i.e., perturbation functions depend only on $\mathbf{q}$, then the perturbed marginal distribution of $\mathbf{q}$ is

$$\rho_{\boldsymbol{\lambda}}(\mathbf{q}) = \int \rho_{\boldsymbol{\lambda}}(\mathbf{q},\mathbf{q}')d\mathbf{q}' = \int e^{\boldsymbol{\lambda}\cdot\mathbf{f}(\mathbf{q})-\psi(\boldsymbol{\lambda})}\rho(\mathbf{q},\mathbf{q}')d\mathbf{q}' = e^{\boldsymbol{\lambda}\cdot\mathbf{f}(\mathbf{q})-\psi(\boldsymbol{\lambda})}\rho(\mathbf{q}). \quad (25)$$

This is the same distribution as Eq. (3). Therefore, our perturbational formulation of PCA is valid without any modification in explicit water simulation if we only perturb the biomolecular coordinates.

Second, sufficient conformational sampling is required because insufficient conformational sampling results in poor estimations of the principal components. This problem has been intensively challenged at least by three different approaches. The first is employment of more efficient sampling algorithms such as extended ensemble algorithms [33,34], the second is the development of the algorithm for improving the parallel scalability of the cluster computer for MD simulation [35,36], and the last is design of fast special-purpose hardware for MD simulation [37,38]. By combining these approaches, the insufficient conformational sampling problem may be solved in the near future. At that time, analysis method of the MD simulation data will become more important.

Third, computational feasibility of diagonalization of the covariance matrix is a problem in PCA. The atom number N of an ordinary protein is 10^3-10^4. If we perturb all the atomic potential energy terms in the protein molecule, then the size of the covariance matrix is $N^2 \sim 10^6-10^8$. Such a large matrix is difficult to diagonalize with the existing computational power. Instead of perturbing each atomic potential energy term, we can perturb some potential energy terms at a time. For example, we can consider groups of atoms such as amino acids or bases, then perturb the intergroup nonbonded potential energy terms simultaneously. If we consider amino acid as one such group, then the group size, i.e., the amino acid number N_a is 10^2-10^3 and the size of the covariance matrix is ${N_a}^2 \sim 10^4-10^6$. Thus the diagonalization is feasible. In this analysis, we can identify the important combinations of the intergroup interactions contributing to conformational distribution change. Note that Kong *et al.* [39] used residue-based interaction-correlation matrix to study the signal-transduction mechanism of rhodopsin. In this respect, our PEPCA method is considered to be a covariance matrix counterpart of their interaction correlation matrix analysis. As another way to reduce the matrix size, we can use the Gram matrix diagonalization instead of the covariance matrix. This is because the formal equivalence between the PCA using perturbation functions and the kernel PCA [40] holds as shown in Appendix C. Since the Gram matrix depends only on the sample data size, the Gram matrix diagonalization may be useful when the number of the perturbation functions is larger than the sample data size. This equivalence between the PCA using perturbation functions and the kernel PCA may also provide the physical meaning to some dimension reduction methods. It is known that several dimension reduction methods, such as metric multidimensional scaling (metric MDS [41], also known as principal coordinate analysis [3,42]), Isomap [43], Laplacian eigenmap [44], and locally linear embedding (LLE) [45] are interpreted as kernel PCA [46,47]. Therefore, it may be interesting to interpret these dimensional reduction methods with our perturbational formulation, because the perturbation may have a clearer physical meaning than the kernel function. We also note that our perturbational formulation of PCA provides the clearer limitation that is defined by the second order approximation of the Kullback-Leibler divergence in comparison with the kernel PCA.

Finally, we estimate the Kullback-Leibler divergence by the perturbation from the unperturbed equilibrium state, i.e., a perturbation estimator only reweights the samples from the unperturbed distribution. Therefore, if the perturbation changes the conformational distribution into unsampled conformations in unperturbed equilibrium state, then the perturbation estimation is invalid. Recently, it has been observed that some proteins "sample" the functional conformations under the unperturbed conformational fluctuation, which is known as a "pre-existing" behavior [2,48]. As demonstrated in Sec. III, our perturbational formulation of PCA is well suited for pre-existing behavior. If a molecular function follows the pre-existing behavior, then the principal components identify the functional substates, and their detailed atomic interactions can be obtained from their eigenvectors. From the components of the eigenvectors, we may be able to identify the natural perturbation targets for molecular functions, such as the ligand binding sites, which induce the large conformational distribution change [16]. Thus, while we need more investigations for larger molecules, PCA can be applied, by carefully selecting the perturbation functions, not only to identify the molecular conformational fluctuation but also to predict the conformational distribution change by the perturbation beyond the limitation of the previous methods.

ACKNOWLEDGMENTS

We thank Mitsunori Takano, Hironori Nakamura, Makoto Taiji, and Noriaki Okimoto for valuable discussions. We are also thankful for the computational resources of the RIKEN Super Combined Cluster (RSCC). This research was supported by the Center for Developmental Biology (CDB) (H.R.U.) and by the Japan Society for the Promotion of Science for Young Scientists 17-4169 (T.J.K).

APPENDIX A: EXPECTATION PARAMETER REPRESENTATION OF THE KULLBACK-LEIBLER DIVERGENCE

Equation (6) indicates that $D(\rho_{\boldsymbol{\lambda}}\|\rho)$ is the Legendre transformation of $\psi(\boldsymbol{\lambda})$. Therefore, $\langle\mathbf{f}\rangle_{\boldsymbol{\lambda}}$ and $\boldsymbol{\lambda}$ have a one-to-one correspondence. As a result, we can use $\langle\mathbf{f}\rangle_{\boldsymbol{\lambda}}$ for specifying the perturbed distribution $\rho_{\boldsymbol{\lambda}}(\mathbf{q})$ instead of $\boldsymbol{\lambda}$. In this respect, $\langle\mathbf{f}\rangle_{\boldsymbol{\lambda}}$ are called expectation parameters [20]. Because of Cramér's theorem in large deviation theory [23,26], the Legendre transformation of the cumulant generating function $\psi(\boldsymbol{\lambda})$ is also a rate function $\phi(\langle\mathbf{f}\rangle_{\boldsymbol{\lambda}})$. Therefore, the equality

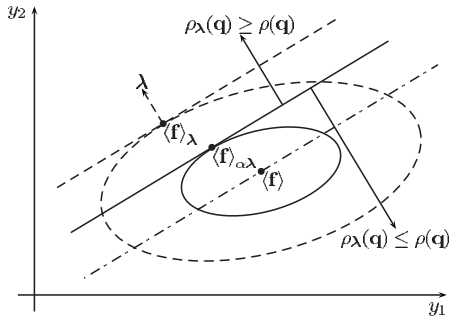

FIG. 3. Hyperplanes determining the probability change of $\mathbf{q}$ by the perturbation $\boldsymbol{\lambda}$ and contours of the Kullback-Leibler divergence. The solid line shows the hyperplane $\boldsymbol{\lambda}\cdot\mathbf{y}-\psi(\boldsymbol{\lambda})=0$ which separates the increases or decreases of the probability change of $\mathbf{q}$ by the perturbation $\boldsymbol{\lambda}$. The solid and broken ellipses show the contours of the Kullback-Leibler divergence of $\phi(\mathbf{y})=C(\rho,\rho_{\boldsymbol{\lambda}})$ and $\phi(\mathbf{y})=D(\rho_{\boldsymbol{\lambda}}\|\rho)$, respectively.

$$\phi(\langle \mathbf{f} \rangle_{\boldsymbol{\lambda}}) = D(\rho_{\boldsymbol{\lambda}} \| \rho) \tag{A1}$$

holds. This relation between the rate function and the Kullback-Leibler divergence is a direct consequence of the contraction principle in large deviation theory [23,26], which states that the rate function is obtained by minimization of the Kullback-Leibler divergence $D(\rho'\|\rho)$ under the probability distribution $\rho'(\mathbf{q})$ which has given averages of statistics $\mathbf{f}(\mathbf{q})$. Since the exponential family [Eq. (3)] is the solution of such minimization, the above equality holds. In this interpretation, $\boldsymbol{\lambda}$ indicate the Lagrange multipliers of the constraints for the averages.

Equation (3) indicates that the probability change of $\mathbf{q}$ by the perturbation $\boldsymbol{\lambda}$ is determined by $\boldsymbol{\lambda}\cdot\mathbf{f}(\mathbf{q})-\psi(\boldsymbol{\lambda})$, and $\boldsymbol{\lambda}\cdot\mathbf{y}-\psi(\boldsymbol{\lambda})=0$ defines the hyperplane in which the probability of $\mathbf{q}$ does not change by the perturbation $\boldsymbol{\lambda}$. We can show that the inequality

$$\boldsymbol{\lambda}\cdot\langle \mathbf{f} \rangle \leqslant \psi(\boldsymbol{\lambda}) \leqslant \boldsymbol{\lambda}\cdot\langle \mathbf{f} \rangle_{\boldsymbol{\lambda}} \tag{A2}$$

holds. The left inequality is from Eq. (4) with Jensen's inequality. The right inequality follows Eq. (6) with the nonnegativity of the Kullback-Leibler divergence [Eq. (5)]. Note that this inequality is considered to be a multidimensional perturbation version of the Gibbs-Bogoliubov inequality [49]. The inequality (A2) shows that the hyperplane $\boldsymbol{\lambda}\cdot\mathbf{y}-\psi(\boldsymbol{\lambda})=0$ is located between $\boldsymbol{\lambda}\cdot(\mathbf{y}-\langle\mathbf{f}\rangle)=0$ and $\boldsymbol{\lambda}\cdot(\mathbf{y}-\langle\mathbf{f}\rangle_{\boldsymbol{\lambda}})=0$. Because $\boldsymbol{\lambda}$ is a gradient of $\phi(\mathbf{y})$ at $\mathbf{y}=\langle\mathbf{f}\rangle_{\boldsymbol{\lambda}}$, $\boldsymbol{\lambda}\cdot(\mathbf{y}-\langle\mathbf{f}\rangle_{\boldsymbol{\lambda}})=0$ is the tangent hyperplane of the contour of $\phi(\mathbf{y})$ at $\mathbf{y}=\langle\mathbf{f}\rangle_{\boldsymbol{\lambda}}$. The inequality (A2) also indicates that for a certain $0\leqslant\alpha(\boldsymbol{\lambda})\leqslant 1$, the equality

$$\psi(\boldsymbol{\lambda}) = \boldsymbol{\lambda}\cdot\langle \mathbf{f} \rangle_{\alpha(\boldsymbol{\lambda})\boldsymbol{\lambda}} \tag{A3}$$

holds. We can show that this equality leads to

$$D(\rho_{\alpha(\boldsymbol{\lambda})\boldsymbol{\lambda}} \| \rho) = D(\rho_{\alpha(\boldsymbol{\lambda})\boldsymbol{\lambda}} \| \rho_{\boldsymbol{\lambda}}) \equiv C(\rho, \rho_{\boldsymbol{\lambda}}), \tag{A4}$$

where $C(\rho,\rho_{\boldsymbol{\lambda}})$ is known as the Chernoff information [24,50,51]. Therefore, $\boldsymbol{\lambda}\cdot\mathbf{y}-\psi(\boldsymbol{\lambda})=\boldsymbol{\lambda}\cdot(\mathbf{y}-\langle\mathbf{f}\rangle_{\alpha(\boldsymbol{\lambda})\boldsymbol{\lambda}})=0$ is the tangent hyperplane of the contour of $\phi(\mathbf{y})=C(\rho,\rho_{\boldsymbol{\lambda}})$ at $\mathbf{y}=\langle\mathbf{f}\rangle_{\alpha(\boldsymbol{\lambda})\boldsymbol{\lambda}}$. The relationship of the hyperplanes and the contours of the Kullback-Leibler divergence is summarized in Fig. 3.

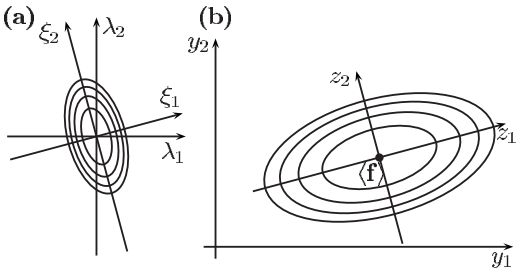

FIG. 4. Contours of the Kullback-Leibler divergence and eigenvectors. Within the second order approximation of the Kullback-Leibler divergence, the contours of the Kullback-Leibler divergence make ellipsoids and eigenvectors corresponding to the principal axes of ellipsoids [Eqs. (8), (A6), and (A8)]. (a) $\boldsymbol{\lambda}$ (natural parameters in the exponential family) representation of the Kullback-Leibler divergence. The Kullback-Leibler divergence in the second order approximation with $\boldsymbol{\lambda}$ representation is Eq. (8). Axes ξ_1 and ξ_2 correspond to the first and second eigenvectors, respectively. $\boldsymbol{\lambda}=0$ corresponds to the unperturbed distribution. (b) $\langle\mathbf{f}\rangle_{\boldsymbol{\lambda}}$ (expectation parameters in the exponential family) representation of the Kullback-Leibler divergence, i.e., rate function $\phi(\langle\mathbf{f}\rangle_{\boldsymbol{\lambda}})$ [Eq. (A1)]. The second order approximation of the Kullback-Leibler divergence with $\langle\mathbf{f}\rangle_{\boldsymbol{\lambda}}$ representation is Eq. (A6). Axes z_1 and z_2 correspond to the first and second principal components, respectively [Eq. (A8)]. $\mathbf{y}=\langle\mathbf{f}\rangle$ corresponds to the unperturbed distribution.

Within the second order approximation of the cumulant generating function $\psi(\boldsymbol{\lambda})$, $\boldsymbol{\lambda}$ can be expressed by $\langle\mathbf{f}\rangle_{\boldsymbol{\lambda}}$ as

$$\boldsymbol{\lambda} \approx \mathbf{C}^{-1}(\langle \mathbf{f} \rangle_{\boldsymbol{\lambda}} - \langle \mathbf{f} \rangle). \tag{A5}$$

With this, Eq. (7) can be represented as

$$\phi(\langle \mathbf{f} \rangle_{\boldsymbol{\lambda}}) = D(\rho_{\boldsymbol{\lambda}} \| \rho) \approx \frac{1}{2}(\langle \mathbf{f} \rangle_{\boldsymbol{\lambda}} - \langle \mathbf{f} \rangle)^T \mathbf{C}^{-1}(\langle \mathbf{f} \rangle_{\boldsymbol{\lambda}} - \langle \mathbf{f} \rangle). \tag{A6}$$

Note that

$$\sqrt{(\langle \mathbf{f} \rangle_{\boldsymbol{\lambda}} - \langle \mathbf{f} \rangle)^T \mathbf{C}^{-1}(\langle \mathbf{f} \rangle_{\boldsymbol{\lambda}} - \langle \mathbf{f} \rangle)} \tag{A7}$$

is known as the Mahalanobis distance [3,41]. With Eq. (14), Eq. (A6) can be represented as

$$\phi(\langle \mathbf{f} \rangle_{\boldsymbol{\lambda}}) \approx \frac{1}{2}\langle \mathbf{g} \rangle_{\boldsymbol{\xi}}^T \mathbf{U}^T \mathbf{C}^{-1} \mathbf{U} \langle \mathbf{g} \rangle_{\boldsymbol{\xi}} \approx \frac{1}{2}\sum_{i=1}^{M} \frac{\langle g_i \rangle_{\boldsymbol{\xi}}^2}{\sigma_i^2}. \tag{A8}$$

With Eqs. (8), (A6), and (A8), contours of the Kullback-Leibler divergence with $\boldsymbol{\lambda}$ and $\langle\mathbf{f}\rangle_{\boldsymbol{\lambda}}$ representation are shown in Fig. 4.

APPENDIX B: PERTURBATIONAL FORMULATION OF CARTESIAN PCA AND DPCA

We consider perturbational formulations of Cartesian PCA and dPCA. In Cartesian PCA, PCA is performed in Cartesian coordinate space such as the N_C C_α atoms of the protein molecule

$$\mathbf{f}(\mathbf{q}) = (q_1, \ldots, q_{3N_C})^T. \tag{B1}$$

Then, the perturbation term in Eq. (2) is represented as

$$-k_BT\sum_{i=1}^{M}\lambda_i f_i(\mathbf{q}) = -k_BT\sum_{i=1}^{3N_C}\lambda_i q_i. \tag{B2}$$

This means that the coordinate q_i is perturbed by the constant force $k_BT\lambda_i$. Therefore, the Cartesian PCA can be interpreted as a method for (1) decomposing a given constant forces perturbation [Eq. (B2)] into perturbations that independently contribute to the conformational distribution change or (2) successively finding the constant forces perturbation [Eq. (B2)] that induces the largest conformational distribution change under the constraints Eqs. (10). The former interpretation is already known [14]. However, it is always necessary to pay attention to the frame fitting problem when using the Cartesian PCA.

To avoid the frame fitting problem, dihedral angles $\varphi_1, \ldots, \varphi_{N_d}$ were used in PCA [52]. However, the direct use of the dihedral angle is problematic because of the periodicity of the dihedral angles. dPCA [12,13] solves this periodicity problem by performing PCA in the mapped dihedral angle space

$$\mathbf{f}(\mathbf{q}) = (\cos\varphi_1, \sin\varphi_1, \ldots, \cos\varphi_{N_d}, \sin\varphi_{N_d})^T \tag{B3}$$

instead of the dihedral angle space. Then, the perturbation term in Eq. (2) can be represented as

$$\begin{aligned} -k_BT\sum_{i=1}^{M}\lambda_i f_i(\mathbf{q}) &= -k_BT\sum_{i=1}^{N_d}(\lambda_{2i-1}\cos\varphi_i + \lambda_{2i}\sin\varphi_i) \\ &= -k_BT\sum_{i=1}^{N_d}k_i\cos(\varphi_i - \gamma_i). \end{aligned} \tag{B4}$$

To clarify the physical meaning of the perturbation, we introduced $\mathbf{k}=(k_1, \ldots, k_{N_d})^T$ and $\boldsymbol{\gamma}=(\gamma_1, \ldots, \gamma_{N_d})^T$ as polar coordinates of $\boldsymbol{\lambda}$ such that $(\lambda_{2i-1}, \lambda_{2i})^T=(k_i\cos\gamma_i, k_i\sin\gamma_i)^T$. Since $\boldsymbol{\lambda}$ and $(\mathbf{k}, \boldsymbol{\gamma})$ show one-to-one correspondence, the constraints Eqs. (10) can also be represented by $\mathbf{k}$ and $\boldsymbol{\gamma}$ instead of $\boldsymbol{\lambda}$. For this purpose, we calculate

$$|\boldsymbol{\lambda}|^2 = \sum_{i=1}^{N_d}[(k_i\cos\gamma_i)^2 + (k_i\sin\gamma_i)^2] = |\mathbf{k}|^2 \tag{B5}$$

and if we represent the jth eigenvector $\mathbf{u}_j$ by $\mathbf{k}^{(j)}$ and $\boldsymbol{\gamma}^{(j)}$, then

$$\begin{aligned} \mathbf{u}_j\cdot\boldsymbol{\lambda} &= \sum_{l=1}^{N_d}[(k_l^{(j)}\cos\gamma_l^{(j)})(k_l\cos\gamma_l) + (k_l^{(j)}\sin\gamma_l^{(j)})(k_l\sin\gamma_l)] \\ &= \sum_{l=1}^{N_d}k_l^{(j)}k_l\cos(\gamma_l^{(j)} - \gamma_l). \end{aligned} \tag{B6}$$

With these expressions, the constraints Eqs. (10) are represented as

$$|\mathbf{k}| = \delta, \quad \delta \text{ such that the second order approximation of } D(\rho_{\mathbf{k},\boldsymbol{\gamma}}\|\rho) \text{ is valid,} \tag{B7a}$$

$$\sum_{l=1}^{N_d}k_l^{(j)}k_l\cos(\gamma_l^{(j)} - \gamma_l) = 0, \quad j = 1, \ldots, i-1, \tag{B7b}$$

in terms of $\mathbf{k}$ and $\boldsymbol{\gamma}$. Thus, the dPCA can be interpreted as a method for (1) decomposing a given dihedral angles perturbation [Eq. (B4)] into perturbations that independently contribute to the conformational distribution change or (2) successively finding the dihedral angles perturbation [Eq. (B4)] that induces the largest conformational distribution change under the constraints Eqs. (B7). Above derivation of the perturbational formulation of dPCA also demonstrates the general procedure for inventing a PCA which is free from the frame fitting problem as follows. First, introduce a physically meaningful perturbation which perturbing some internal coordinates. Second, divide the perturbation as the perturbation term in Eq. (2). Finally, perform PCA using $\mathbf{f}(\mathbf{q})$. Introduction of the PEPCA in Sec. II D also follows this procedure.

APPENDIX C: RELATIONSHIP TO THE KERNEL PCA

We noticed a formal equivalence between the PCA using the perturbation functions developed in Sec. II C and the kernel PCA [40], because each methods can be interpreted as the PCA in a mapped space $\mathbf{f}(\mathbf{q})$ (this space is called feature space in the kernel method) instead of $\mathbf{q}$. To show this equivalence, we briefly introduce the kernel PCA in our notation. We consider n point data $(\mathbf{q}_1, \ldots, \mathbf{q}_n)$, and their centered mapped data matrix

$$\tilde{\mathbf{D}} \equiv [\tilde{\mathbf{f}}(\mathbf{q}_1), \ldots, \tilde{\mathbf{f}}(\mathbf{q}_n)], \tag{C1}$$

where centered mapped data is

$$\tilde{\mathbf{f}}(\mathbf{q}_i) \equiv \mathbf{f}(\mathbf{q}_i) - \frac{1}{n}\sum_{l=1}^{n}\mathbf{f}(\mathbf{q}_l). \tag{C2}$$

We represent the centered mapped data matrix $\tilde{\mathbf{D}}$ by singular value decomposition [27] as

$$\tilde{\mathbf{D}} = \sum_{i=1}^{r}\sqrt{n}\sigma_i\mathbf{u}_i\mathbf{v}_i^T, \tag{C3}$$

where r, $\sqrt{n}\sigma_i$, $\mathbf{U}=(\mathbf{u}_1, \ldots, \mathbf{u}_r)$, and $\mathbf{V}=(\mathbf{v}_1, \ldots, \mathbf{v}_r)$ are the rank of $\tilde{\mathbf{D}}$, singular values, left singular vectors, and right singular vectors, respectively. In this representation, the covariance matrix of the mapped data is

$$\mathbf{C} \equiv \frac{1}{n}\tilde{\mathbf{D}}\tilde{\mathbf{D}}^T = \sum_{i=1}^{r}\sigma_i^2\mathbf{u}_i\mathbf{u}_i^T. \tag{C4}$$

$\mathbf{C}$ is an $M\times M$ matrix, whose size depends on the dimension M of the mapped space. The above equation indicates that the eigenvalues and the eigenvectors of $\mathbf{C}$ give σ_i^2 and $\mathbf{u}_i$, respectively. In our PCA using perturbation functions, this diagonalization is performed. On the other hand, in the kernel PCA, the centered Gram matrix $\tilde{\mathbf{G}}$

$$\tilde{\mathbf{G}} \equiv \tilde{\mathbf{D}}^T \tilde{\mathbf{D}} = \sum_{i=1}^{r} n\sigma_i^2 \mathbf{v}_i \mathbf{v}_i^T \tag{C5}$$

is diagonalized instead of the covariance matrix $\mathbf{C}$. $\tilde{\mathbf{G}}$ is a $n \times n$ matrix, whose size depends on the data size n. With Eqs. (C1), (C2), and (C5), the element of the centered Gram matrix $\tilde{G}_{ij}$ can be represented as

$$\tilde{G}_{ij} = \tilde{\mathbf{f}}(\mathbf{q}_i) \cdot \tilde{\mathbf{f}}(\mathbf{q}_j) = \tilde{k}(\mathbf{q}_i, \mathbf{q}_j) = k(\mathbf{q}_i, \mathbf{q}_j) - \frac{1}{n}\sum_{m=1}^{n} k(\mathbf{q}_i, \mathbf{q}_m)$$

$$- \frac{1}{n}\sum_{l=1}^{n} k(\mathbf{q}_l, \mathbf{q}_j) + \frac{1}{n^2}\sum_{l,m=1}^{n} k(\mathbf{q}_l, \mathbf{q}_m), \tag{C6}$$

where we introduced the kernel function $k(\mathbf{q}, \mathbf{q}')$

$$k(\mathbf{q}, \mathbf{q}') \equiv \mathbf{f}(\mathbf{q}) \cdot \mathbf{f}(\mathbf{q}') \tag{C7}$$

and the centered kernel function $\tilde{k}(\mathbf{q}, \mathbf{q}')$

$$\tilde{k}(\mathbf{q}, \mathbf{q}') \equiv \tilde{\mathbf{f}}(\mathbf{q}) \cdot \tilde{\mathbf{f}}(\mathbf{q}'). \tag{C8}$$

Thus, the centered Gram matrix $\tilde{\mathbf{G}}$ [and also centered kernel function $\tilde{k}(\mathbf{q}, \mathbf{q}')$] can be calculated using the kernel function $k(\mathbf{q}, \mathbf{q}')$, and the explicit functional form of $\mathbf{f}(\mathbf{q})$ is not required. As a first selection of the kernel function, the polynomial kernel

$$k(\mathbf{q}, \mathbf{q}') = (\mathbf{q} \cdot \mathbf{q}' + c)^d \tag{C9}$$

and the Gaussian kernel

$$k(\mathbf{q}, \mathbf{q}') = e^{-|\mathbf{q} - \mathbf{q}'|^2/2\sigma^2}, \tag{C10}$$

are often used in the kernel method. In particular, the Gaussian kernel has infinite dimensional feature space. We can see from Eq. (C5), the eigenvalues and the eigenvectors of the centered Gram matrix $\tilde{\mathbf{G}}$ are $n\sigma_i^2$ and $\mathbf{v}_i$, respectively. Therefore, by dividing eigenvalues $n\sigma_i^2$ of $\tilde{\mathbf{G}}$ by data size n, we can obtain the eigenvalue σ_i^2 of $\mathbf{C}$. The eigenvectors to be determined are not $\mathbf{v}_i$ but $\mathbf{u}_i$. From Eq. (C3), $\mathbf{u}_j$ can be represented as

$$\mathbf{u}_j = \frac{\tilde{\mathbf{D}}\mathbf{v}_j}{\sqrt{n\sigma_j}} = \frac{\sum_{i=1}^{n} V_{ij} \tilde{\mathbf{f}}(\mathbf{q}_i)}{\sqrt{n\sigma_j}}. \tag{C11}$$

With this expression, the jth principal component $g_j(\mathbf{q})$ is represented as

$$g_j(\mathbf{q}) \equiv \mathbf{u}_j \cdot \tilde{\mathbf{f}}(\mathbf{q}) = \frac{\sum_{i=1}^{n} V_{ij} \tilde{\mathbf{f}}(\mathbf{q}_i) \cdot \tilde{\mathbf{f}}(\mathbf{q})}{\sqrt{n\sigma_j}} = \frac{\sum_{i=1}^{n} V_{ij} \tilde{k}(\mathbf{q}_i, \mathbf{q})}{\sqrt{n\sigma_j}}. \tag{C12}$$

Thus, in the kernel PCA, the eigenvalues σ_i^2 and the principal components $\mathbf{g}(\mathbf{q})$ can be calculated by the diagonalization of the centered Gram matrix $\tilde{\mathbf{G}}$, which can be evaluated by the kernel function. On the other hand, Eq. (C11) indicates that the eigenvectors $\mathbf{u}_i$ require the explicit functional form of $\mathbf{f}(\mathbf{q})$.

For example, a homogeneous polynomial kernel of degree two, i.e., $c=0$ and $d=2$ in Eq. (C9), is represented as

$$k(\mathbf{q}, \mathbf{q}') = (\mathbf{q} \cdot \mathbf{q}')^2 = \sum_{i=1}^{3N_C} q_i^2 q_i'^2 + 2 \sum_{1 \leqslant i < j \leqslant 3N_C} q_i q_j q_i' q_j'$$

$$= \mathbf{f}(\mathbf{q}) \cdot \mathbf{f}(\mathbf{q}'), \tag{C13}$$

where

$$\mathbf{f}(\mathbf{q}) = (\{q_i^2 | i = 1, \ldots, 3N_C\}, \{\sqrt{2} q_i q_j | 1 \leqslant i < j \leqslant 3N_C\})^T. \tag{C14}$$

In our perturbational formulation of PCA, this perturbation functions $\mathbf{f}(\mathbf{q})$ give the harmonic perturbation around the origin. The polynomial kernel [Eq. (C9)] and the Gaussian kernel [Eq. (C10)] in Cartesian coordinates were applied in the MD simulation [53]. However, using Cartesian coordinates leads to the frame fitting problem, as in the case of the Cartesian PCA. It is desirable to use the invariant kernel function with respect to the overall molecular motion. For this purpose, it may be useful to perform the kernel PCA with a kernel function such as the polynomial kernel [Eq. (C9)] and the Gaussian kernel [Eq. (C10)] with respect to the mapped dihedral angle space [Eq. (B3)] or potential energy term space [Eq. (20)].

[1] S. Hammes-Schiffer and S. J. Benkovic, Annu. Rev. Biochem. **75**, 519 (2006).
[2] K. Henzler-Wildman and D. Kern, Nature (London) **450**, 964 (2007).
[3] I. T. Jolliffe, *Principal Component Analysis*, 2nd ed. (Springer, New York, 2002).
[4] A. Kitao, F. Hirata, and N. Go, Chem. Phys. **158**, 447 (1991).
[5] A. E. García, Phys. Rev. Lett. **68**, 2696 (1992).
[6] A. Amadei, A. B. M. Linssen, and H. J. C. Berendsen, Proteins **17**, 412 (1993).
[7] A. Kitao and N. Go, Curr. Opin. Struct. Biol. **9**, 164 (1999).
[8] H. J. C. Berendsen and S. Hayward, Curr. Opin. Struct. Biol. **10**, 165 (2000).
[9] P. H. Hünenberger, A. E. Mark, and W. F. van Gunsteren, J. Mol. Biol. **252**, 492 (1995).
[10] M. Karplus and T. Ichiye, J. Mol. Biol. **263**, 120 (1996).
[11] R. Abseher and M. Nilges, J. Mol. Biol. **279**, 911 (1998).
[12] Y. Mu, P. H. Nguyen, and G. Stock, Proteins **58**, 45 (2005).
[13] A. Altis, P. H. Nguyen, R. Hegger, and G. Stock, J. Chem. Phys. **126**, 244111 (2007).
[14] M. Ikeguchi, J. Ueno, M. Sato, and A. Kidera, Phys. Rev. Lett. **94**, 078102 (2005).
[15] D. Ming and M. E. Wall, Proteins **59**, 697 (2005).
[16] D. Ming and M. E. Wall, J. Mol. Biol. **358**, 213 (2006).

[17] S. Kullback, *Information Theory and Statistics* (John Wiley & Sons, New York, 1959).
[18] O. Barndorff-Nielsen, *Information and Exponential Families In Statistical Theory* (John Wiley & Sons, Chichester, 1978).
[19] L. D. Brown, *Fundamentals of Statistical Exponential Families: With Applications in Statistical Decision Theory* (Institute of Mathematical Statistics, Hayward, CA, 1986).
[20] S. Amari and H. Nagaoka, *Methods of Information Geometry* (AMS and Oxford University Press, New York, 2000).
[21] H.-O. Georgii, in *Entropy*, edited by A. Greven, G. Keller, and G. Warnecke (Princeton University Press, Princeton, 2003), pp. 37–54.
[22] S. Kullback and R. A. Leibler, Ann. Math. Stat. **22**, 79 (1951).
[23] S. R. S. Varadhan, in *Entropy* [21], pp. 199–214.
[24] T. M. Cover and J. A. Thomas, *Elements of Information Theory*, 2nd ed. (Wiley-Interscience, New York, 2006).
[25] I. N. Sanov, Mat. Sb. **42**, 11 (1957).
[26] A. Dembo and O. Zeitouni, *Large Deviations Techniques and Applications*, 2nd ed. (Springer, New York, 1998).
[27] R. A. Horn and C. R. Johnson, *Matrix Analysis* (Cambridge University Press, Cambridge, 1985).
[28] J. W. Ponder and D. A. Case, Adv. Protein Chem. **66**, 27 (2003).
[29] D. A. Case, T. A. Darden, T. E. Cheatham, III, C. L. Simmerling, J. Wang, R. E. Duke, R. Luo, K. M. Merz, B. Wang, D. A. Pearlman, M. Crowley, S. Brozell, V. Tsui, H. Gohlke, J. Mongan, V. Hornak, G. Cui, P. Beroza, C. Schafmeister, J. W. Caldwell, W. S. Ross, and P. A. Kollman, AMBER8, University of California, San Francisco, 2004.
[30] Y. Duan, C. Wu, S. Chowdhury, M. C. Lee, G. Xiong, W. Zhang, R. Yang, P. Cieplak, R. Luo, T. Lee, J. Caldwell, J. Wang, and P. Kollman, J. Comput. Chem. **24**, 1999 (2003).
[31] http://www.r-project.org/
[32] W. Humphrey, A. Dalke, and K. Schulten, J. Mol. Graphics **14**, 33 (1996).
[33] Y. Iba, Int. J. Mod. Phys. C **12**, 623 (2001).
[34] Y. Okamoto, J. Mol. Graphics Modell. **22**, 425 (2004).
[35] J. C. Phillips, R. Braun, W. Wang, J. Gumbart, E. Tajkhorshid, E. Villa, C. Chipot, R. D. Skeel, L. Kale, and K. Schulten, J. Comput. Chem. **26**, 1781 (2005).
[36] K. J. Bowers, E. Chow, H. Xu, R. O. Dror, M. P. Eastwood, B. A. Gregersen, J. L. Klepeis, I. Kolossváry, M. A. Moraes, F. D. Sacerdoti, J. K. Salmon, Y. Shan, and D. E. Shaw, in Proceedings of the ACM/IEEE Conference on Supercomputing (SC06) (ACM Press, New York, 2006).
[37] M. Taiji, T. Narumi, Y. Ohno, N. Futatsugi, A. Suenaga, N. Takada, and A. Konagaya, in Proceedings of the ACM/IEEE Conference on Supercomputing (SC03) (ACM Press, New York, 2003).
[38] D. E. Shaw, M. M. Deneroff, R. O. Dror, J. S. Kuskin, R. H. Larson, J. K. Salmon, C. Young, B. Batson, K. J. Bowers, J. C. Chao, M. P. Eastwood, J. Gagliardo, J. P. Grossman, C. R. Ho, D. J. Ierardi, I. Kolossváry, J. L. Klepeis, T. Layman, C. McLeavey, M. A. Moraes, R. Mueller, E. C. Priest, Y. Shan, J. Spengler, M. Theobald, B. Towles, and S. C. Wang, Commun. ACM **51**(7), 91 (2008).
[39] Y. Kong and M. Karplus, Structure (London) **15**, 611 (2007).
[40] B. Schölkopf, A. Smola, and K. Müller, Neural Comput. **10**, 1299 (1998).
[41] K. V. Mardia, J. T. Kent, and J. M. Bibby, *Multivariate Analysis* (Academic Press, London, 1979).
[42] J. C. Gower, Biometrika **53**, 325 (1966).
[43] J. B. Tenenbaum, V. de Silva, and J. C. Langford, Science **290**, 2319 (2000).
[44] M. Belkin and P. Niyogi, Neural Comput. **15**, 1373 (2003).
[45] S. T. Roweis and L. K. Saul, Science **290**, 2323 (2000).
[46] C. K. I. Williams, Mach. Learn. **46**, 11 (2002).
[47] J. Ham, D. D. Lee, S. Mika, and B. Schölkopf, in *Proceedings of the Twenty-First International Conference on Machine Learning* (ACM Press, New York, 2004), pp. 369–376.
[48] K. Gunasekaran, B. Ma, and R. Nussinov, Proteins **57**, 433 (2004).
[49] C. Chipot and A. Pohorille, in *Free Energy Calculations: Theory and Applications in Chemistry and Biology*, edited by C. Chipot and A. Pohorille (Springer, Berlin, 2007) pp. 33–75.
[50] H. Chernoff, Ann. Math. Stat. **23**, 493 (1952).
[51] S. Sinanović and D. H. Johnson, Signal Process. **87**, 1326 (2007).
[52] D. M. F. van Aalten, B. L. de Groot, J. B. C. Findlay, H. J. C. Berendsen, and A. Amadei, J. Comput. Chem. **18**, 169 (1997).
[53] X.-w. Chen and J. Chen, in Proceedings of the IEEE International Joint Conference on Neural Networks (IJCNN'05) (IEEE Press, New York, 2005), Vol. 1, pp. 521–526.